Human ES cell-derived neural rosettes reveal a functionally distinct early neural stem cell stage

Yechiel Elkabetz,[1,2] Georgia Panagiotakos,[2] George Al Shamy,[2] Nicholas D. Socci,[3] Viviane Tabar,[2] and Lorenz Studer[1,2,4]

[1]Developmental Biology Program, Sloan-Kettering Institute, New York, New York 10021, USA; [2]Division of Neurosurgery, Sloan-Kettering Institute, New York, New York 10021, USA; [3]Computational Biology Center, Sloan-Kettering Institute, New York, New York 10021, USA

Neural stem cells (NSCs) yield both neuronal and glial progeny, but their differentiation potential toward multiple region-specific neuron types remains remarkably poor. In contrast, embryonic stem cell (ESC) progeny readily yield region-specific neuronal fates in response to appropriate developmental signals. Here we demonstrate prospective and clonal isolation of neural rosette cells (termed R-NSCs), a novel NSC type with broad differentiation potential toward CNS and PNS fates and capable of in vivo engraftment. R-NSCs can be derived from human and mouse ESCs or from neural plate stage embryos. While R-NSCs express markers classically associated with NSC fate, we identified a set of genes that specifically mark the R-NSC state. Maintenance of R-NSCs is promoted by activation of SHH and Notch pathways. In the absence of these signals, R-NSCs rapidly lose rosette organization and progress to a more restricted NSC stage. We propose that R-NSCs represent the first characterized NSC stage capable of responding to patterning cues that direct differentiation toward region-specific neuronal fates. In addition, the R-NSC-specific genetic markers presented here offer new tools for harnessing the differentiation potential of human ESCs.

[*Keywords*: Human embryonic stem cells; neural patterning; neural stem cells; neuronal specification]

Supplemental material is available at http://www.genesdev.org.

Received September 17, 2007; revised version accepted November 21, 2007.

Neural stem cells (NSCs) are defined by their ability to clonally give rise to the three major CNS lineages: neurons, astrocytes, and oligodendrocytes. The in vitro isolation and propagation of NSCs from the developing and adult CNS has provided an essential tool to study neural precursor biology and lineage differentiation potential (Gage 2000). Much attention has been focused on the factors directing the expansion and differentiation of NSCs in vitro. These studies demonstrated that single factors act instructively to specify neuronal versus glial fate choice (Johe et al. 1996). Two major challenges have limited the use of NSCs to study neural differentiation and to develop cell-based strategies for brain repair: First, under most growth conditions, NSCs show increased gliogenic bias and concomitant loss of neurogenic potential in culture. Second, in vitro expanded NSCs cannot be regionally specified in response to developmental patterning cues. For example, SHH/RA or SHH/FGF8 treatment induce motoneuron and midbrain dopamine neurons, respectively, in neural plate explants (Roelink et al. 1995; Ye et al. 1998) and embryonic stem cell (ESC) progeny (Wichterle et al. 2002; Barberi et al. 2003) but not in cultured NSCs (Caldwell et al. 2001; Jain et al. 2003).

Recent work has shown improved neurogenic potential of NSCs after long-term culture (Conti et al. 2005), although potential for regional specification was not addressed. Studies in mouse ESCs suggested the existence of FGF2/LIF-responsive primitive NSCs (Tropepe et al. 2001). However, these cells exhibit ESC-like differentiation potential in chimeric mice and cannot be maintained without progressing toward a "definitive" NSC stage with limited differentiation potential. Therefore, despite the contribution of these recent studies the isolation of NSCs with true self-renewal and full patterning and differentiation potential has remained elusive.

During neural differentiation human ESCs (hESCs) undergo morphogenetic events characterized by the formation of radially organized columnar epithelial cells termed "neural rosettes" (Zhang et al. 2001; Perrier et al. 2004). These structures comprise cells expressing early neuroectodermal markers such as Pax6 and Sox1 and are capable of differentiating into various region-specific neuronal and glial cell types in response to appropriate developmental cues (Perrier et al. 2004; Li et al. 2005).

[4]**Corresponding author.**
E-MAIL studerl@mskcc.org; FAX (212) 717-3642.
Article is online at http://www.genesdev.org/cgi/doi/10.1101/gad.1616208.

The broad differentiation potential is unique to early rosette stage cells and lost upon further in vitro proliferation. Similar differential competency to patterning signals is observed in neural development comparing neural precursors at the neural plate stage exhibiting broad patterning potential versus neural precursors emerging after neural tube closure (Jessell 2000).

A key question remains as to whether early rosette stage cells contain NSCs that can be prospectively isolated and maintained in vitro while retaining their broad differentiation potential. We and others have shown previously that hESC-derived neural rosettes can be proliferated in the presence of FGF2/EGF, giving rise to precursor cells that maintain expression of NSC markers such as Sox1, Sox2, and nestin, but lack epithelial organization (Conti et al. 2005; Tabar et al. 2005; Shin et al. 2006). We further demonstrated that upon transplantation these cells were capable of integrating into the adult SVZ and contributing to olfactory neurogenesis in a manner similar to host adult rodent NSCs (Tabar et al. 2005). The stem cell characteristics of ESC-derived NSCs have been further demonstrated by clonal analysis in vitro (Barberi et al. 2003). However, there is no evidence that in vitro expanded ESC-derived NSCs can be regionally specified in a manner similar to rosette stage cells.

Here we demonstrate that hESC-derived rosettes represent a novel type of NSCs that can be prospectively isolated, regionally specified, and expanded in vitro without losing rosette properties. By default, neural rosettes adopt anterior CNS characteristics, including expression of Foxg1b (BF1) (Tao and Lai 1992). However, prospective isolation of these $BF1^+$ rosettes using Forse1, a marker of stem and precursor cells specific to anterior CNS fate, demonstrated respecification toward caudal fates, including spinal motoneurons or midbrain dopamine neurons. The stem cell nature of rosettes was assessed by clonal analysis demonstrating rosette reformation and patterning from single-cell progeny. While rosette stage cells express the currently known NSC markers, we identified a unique set of genes selectively expressed in rosette stage cells. Furthermore, rosette stage cells exhibit distinct growth requirements and differentiation potential toward both CNS and PNS fates. Finally, we demonstrate that in addition to hESCs, both mouse ESCs and primary tissue at the neural plate stage can serve as a source of neural rosettes. We propose that neural rosettes represent a novel NSC type distinct from currently characterized NSC stages. The unique differentiation potential of rosette cells yields improved access to therapeutically relevant neuron types. Insights from our study on the molecular mechanisms controlling rosette state should enhance basic understanding of NSC biology.

Results

hESC-derived neural rosettes adopt polarized neuroepithelial structures of anterior CNS fate

The morphogenetic events underlying rosette induction and CNS regionalization, and the relationship of rosettes and NSC biology are poorly understood. To address these questions we monitored neural induction and rosette formation in hESC cultures on neural-inducing MS5 stroma (Barberi et al. 2003; Perrier et al. 2004) and upon neural induction using a serum-free embryoid body (SFEB) culture protocol (Zhang et al. 2001; Watanabe et al. 2005). Gene expression analysis confirmed the progressive loss of pluripotency markers such as Nanog, and an increase in the expression of markers defining early neural fate (Fig. 1A). Progressive neural fate specification was paralleled by an increase in the expression of markers defining anterior CNS identity at the expense of caudal markers (Fig. 1B). These data demonstrate that in the absence of extrinsic patterning cues neural rosettes acquire markers of anterior neural ectoderm.

The formation of neural rosettes (Supplemental Fig. 1) was initiated by the acquisition of cell polarity in hESC progeny illustrated by the redistribution of ZO-1, a tight junction protein (Itoh et al. 1993) expressed evenly on the surface of undifferentiated hESCs (Fig. 1C). We observed that asymmetric apical localization of ZO-1 is a key feature of neural induction (Fig. 1D,E) whereby ZO-1 is colocalized with the neuroepithelial marker N-cadherin (N-cad) at adherens junctions. Distribution of the stem cell marker CD133 similarly became restricted to the apical membranes during neural induction (Fig. 1F). Cell polarity within rosettes was paralleled by a functional asymmetry characterized by the specific distribution of cell nuclei undergoing M phase. While all cells within rosettes proliferated and incorporated BrdU, M-phase cells marked by Phospho-Histone H3 (PH3) expression were restricted to the luminal zone of rosettes (Fig. 1G). Most rosette cells expressed Pax6, while a subset of these cells coexpressed 3CB2 (Fig. 1H), a marker of radial glia (Prada et al. 1995; Conti et al. 2005). Immunocytochemical analyses confirmed the neural stem cell, neuroepithelial, and anterior CNS character of hESC-derived neural rosettes (Fig. 1I–K). Expression of NSC markers was maintained after FGF2/EGF expansion of neural rosette progeny (Tabar et al. 2005). These FGF2/EGF expanded cells match marker expression and functional properties of symmetrically dividing NSC populations (NS cells) (Conti et al. 2005) described previously, and are defined in the context of this study as $NSCs^{FGF2/EGF}$. While $NSCs^{FGF2/EGF}$ express NSC and radial glial markers comparable with rosette stage cells (Fig. 1L,M), $NSCs^{FGF2/EGF}$ show decreased expression of BF1 and a complete loss of epithelial organization and ZO-1 expression (Fig. 1N,O).

Forse1 as a marker for the prospective isolation and clonal derivation of anterior neural rosette cells

We next tested whether neural rosette cells exhibit NSC properties similar to those described for $NSC^{FGF2/EGF}$ cultures (Conti et al. 2005; Tabar et al. 2005). To this end we developed a strategy aimed at the prospective isolation of putative rosette stage NSCs. Cultures of early hESC-derived neural rosettes are not homogenous and can contain differentiated neurons, neural crest deriva-

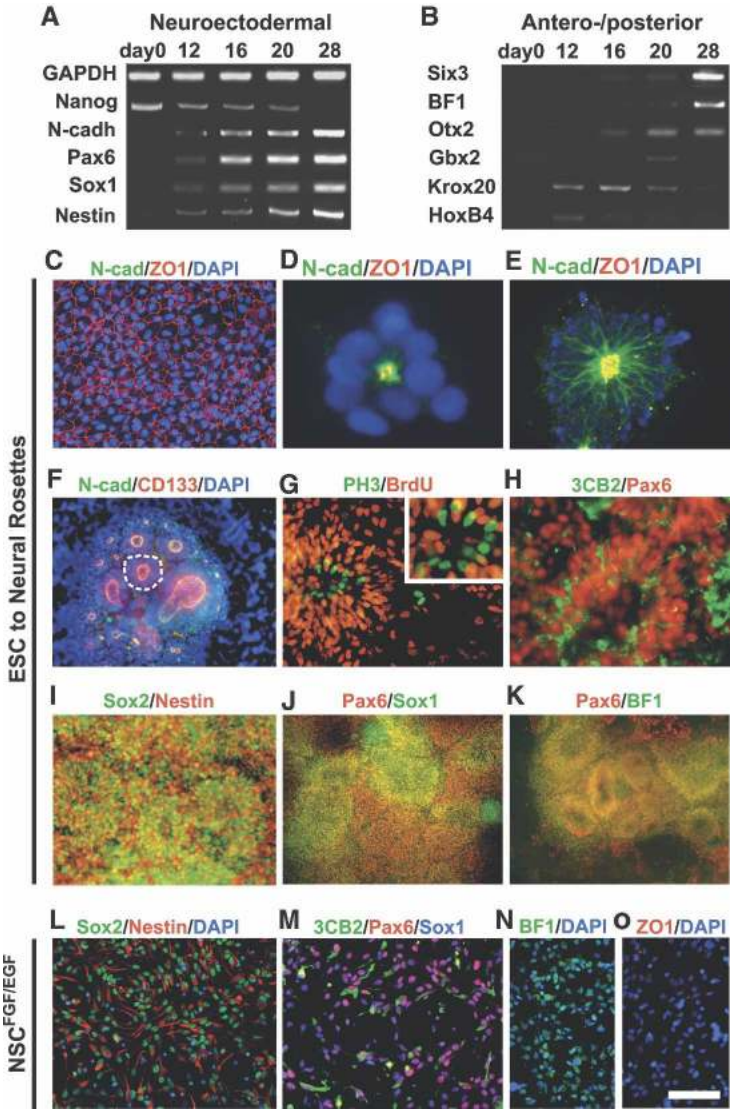

Figure 1. hESC-derived neural rosettes adopt polarized neuroepithelial structures of anterior CNS fate. (*A*) RT–PCR analysis during neural rosette formation for neurectodermal (Pax6 and Sox1), neuroepithelial (N-cad), and neural precursor (Nestin) markers, as well as markers of undifferentiated hESCs (Nanog). (*B*) RT–PCR analysis for anterior CNS markers (BF1, Six3, and Otx2) and markers of posterior CNS fate (Gbx2, Krox20, and Hoxb4). (*C*) Immunocytochemistry for tight junction protein ZO-1 in undifferentiated hESCs, in day 12 rosettes (*D*), and in day 16 rosettes colocalized with N-cad (*E*). (*F*) Immunocytochemistry for CD133 and N-cad. Dashed line outlines a single rosette with an average diameter of ~100 µm. (*G*) Immunocytochemistry for PH3 and BrdU. Evidence of interkinetic nuclear migration. (*H*) Expression of Pax6 and the radial glia marker 3CB2. Immunocytochemistry in hESC-derived rosettes for markers of NSCs (Nestin and Sox2; *I*), neuroepithelial cells (Pax6 and Sox1; *J*), and anterior fate (Pax6 and BF1; *K*). Immunocytochemistry in NSCs$^{FGF2/EGF}$ for markers of NSCs (Nestin and Sox2; *L*), radial glia and neuroepithelial cells (Pax6, 3CB2, and Sox1; *M*), and anterior fate (BF1; *N*, and ZO-1; *O*). The morphological progression to rosette and NSCs$^{FGF2/EGF}$ state is presented in Supplemental Figure 1. Bar in *O* corresponds to 12.5 µm in *D*, 35 µm in *G* (*inset*), 50 µm in *E* and *H*, 67 µm in *C* and *G*, 100 µm in *I* and *L–N*, 125 µm in *F*, and 200 µm in *J* and *K*.

tives, nonneural derivatives, or undifferentiated hESCs. Forse1 was originally isolated as an antibody recognizing a surface epitope expressed in neuroepithelial cells derived upon RA-induction of the human embryonal carcinoma cell line NT2D1 (Tole et al. 1995). A recent study reported Forse1 expression in a subset of hESC-derived neural progeny (Pruszak et al. 2007). We observed that hESC-derived neural rosettes show a progressive increase in Forse1 expression, labeling cells within N-cad$^+$ rosettes (Fig. 2A). Dissociation of neural rosettes revealed that Forse1 expression is restricted to nestin$^+$ cells and not expressed in β3-Tubulin$^+$ neurons (Fig. 2B,C). Additional characterizations of Forse1 expression are presented in Supplemental Figures 2–5.

Clonal analysis of prospectively isolated rosette cells was performed using a constitutively eGFP-expressing hESC line (RU-01eGFP) (James et al. 2006). Forse1$^+$/N-cad$^+$ cells were isolated via fluorescence-activated cell sorting (FACS) from RU-01eGFP and plated at clonal dilution on stage-matched rosette cells derived from a non-GFP hESC line (WA-09). Single -cell-derived eGFP$^+$ clones were marked, and proliferated for 8 d in the presence of SHH/FGF8 (Perrier et al. 2004), passaged, and analyzed after an additional 8–21 d of in vitro expansion. These data showed that single Forse1$^+$ rosette stage cells can generate new rosettes (Fig. 2D). However, not all rosettes were positive for Forse1 (Fig. 2E) and purified Forse1$^-$ cells were also capable of rosette formation (Supplemental Fig. 6). The main difference between Forse1$^+$ and Forse1$^-$ rosettes was expression of BF1. We found that virtually all hESC-derived Forse1$^+$ cells at the rosette stage coexpress the forebrain marker BF1 (Fig. 2H). These results are compatible with data in mouse development where Forse1 predominantly marks forebrain precursor cells (Tole et al. 1995).

Anterior neural rosettes can be respecified toward caudal fates

The prospective isolation of Forse1$^+$ and Forse1$^-$ cells offers the possibility to directly compare the differentia-

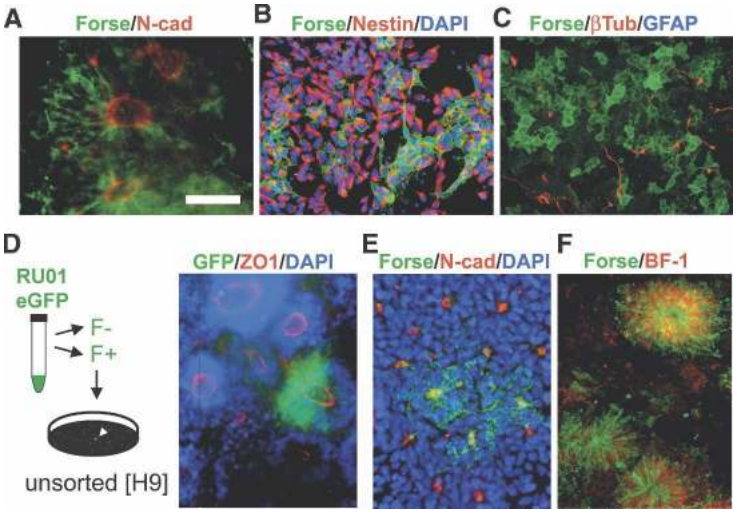

Figure 2. Forse1 is a novel NSC marker for the prospective isolation of anterior neural rosette cells (*A*). Immunocytochemistry for Forse1 in N-cad$^+$ rosettes. Forse1 and Nestin (NSC marker) (*B*) and Forse1 and β3-tubulin (neuronal marker) (*C*) staining in dissociated rosette stage cells. (*D*, *left* panel) Forse1$^+$/N-cad^{high} rosette stage cells were isolated from RU-01eGFP and replated at single-cell density on stage-matched high-cell-density rosette cells from H9 (WA-09). (*Right* panel) Representative image showing clonally derived ZO-1$^+$/eGFP$^+$ rosette. (*E*) Immunocytochemistry for Forse1 and N-cad demonstrates the presence of Forse1$^+$ and Forse1$^-$ rosettes. (*F*) Forse1 colocalization with the telencephalic marker BF1. Bar in *A* corresponds to 50 µm in *A–C* and *E*, 75 µm in *D*, and 100 µm in *F*.

tion potential of rosettes expressing anterior versus posterior fate markers. To this end hESC-derived rosette progeny was isolated at P1 (day 25 of differentiation). Cells were sorted into Forse1$^+$/N-cad^{high} and Forse1$^-$/N-cad^{high} populations and replated in the presence of defined patterning molecules known to direct spinal motoneuron and midbrain dopamine neuron differentiation (Fig. 3A,B). Induction of HB9$^+$ spinal motoneurons (SHH/RA) and En1$^+$ midbrain precursors (SHH/FGF8) was observed in both Forse1$^-$ and Forse1$^+$ rosette cells although Forse1$^-$ R-NSCs were significantly more efficient at generating these caudal neuron types. Importantly, however, cells at the NSC$^{FGF2/EGF}$ stage did not yield any HB9$^+$ motoneurons and minimal numbers of En1$^+$ precursors (Fig. 3A,B). These data demonstrate that neural rosette stage cells can undergo AP specification, and that expression of BF1 at the rosette stage does not irreversibly mark forebrain committed cells. Our findings on patterning BF1$^+$ rosette stage cells were further confirmed in clonal populations of Forse1$^+$ cells derived from RU1-eGFP plated onto unmarked H9-derived rosette stage cells (Fig. 3A,B, insets). Adoption of caudal markers in anterior rosette stage cells in response to RA was monitored by loss of Forse1 and BF1 expression and a concomitant increase in the expression of caudal markers such as HoxB4 (Supplemental Fig. 7). Expression of BF1 in all Forse1$^+$ rosette stage cells, gradual loss of Forse1 and BF1 expression, clonal analyses, and the lack of significant cell death during RA patterning (data not shown) strongly support the hypothesis that RA acts on hESC-derived rosettes via respecification of anterior cells rather than the expansion of a rare putative caudal cell population.

Differentiation of neural rosette progeny in the absence of caudalizing factors but in the presence of ventral and dorsal patterning cues such as SHH or Wnt3A led to the induction of markers compatible with ventral forebrain fate and the emergence of GABA$^+$ neurons (Fig. 3C) and cells expressing dorsal markers such as Msx1 (Fig. 3D). Neural rosettes could also be directed toward astrocytic or oligodendrocytic fates (Fig. 3E) following previously published protocols (Perrier et al. 2004). The capacity for neurosphere formation (Fig. 3F) was comparable in rosette and NSC$^{FGF2/EGF}$ populations. However, particularly among NSC$^{FGF2/EGF}$ stage cells, Forse1$^+$ cells were more efficient at neurosphere formation than Forse1$^-$ cells.

In vivo survival of rosette-derived neuronal subtypes was demonstrated upon transplantation into the adult rat CNS. Rosette-derived motoneuron cultures grafted into the ventral spinal cord yielded ChAT$^+$/HoxA5$^+$ motoneurons 6 wk after transplantation. Human identity was confirmed by expression of human nuclear antigen (Fig. 3G, left panel). Rosette-derived dopamine neurons cultures were grafted into the adult rat striatum and analyzed for coexpression of human nuclear antigen and tyrosine-hydroxylase (Fig. 3G, right panel). The transplantation data provided clear evidence for survival and in vivo phenotype maintenance of rosette-derived dopamine neurons. Our in vitro data (Fig. 3A) showed that NSCs$^{FGF2/EGF}$ are unable to generate spinal motoneuron and midbrain dopamine neuron in response to patterning cues. Transplantation of NSCs$^{FGF2/EGF}$ into the adult rat striatum confirmed absence of motoneuronal and dopaminergic progeny in vivo while overall neuronal differentiation was not compromised (Fig. 3H).

Our data on the clonal derivation and multilineage differentiation of rosettes are indicative of NSC potential. The capacity of rosettes to undergo neural patterning in response to appropriate extrinsic cues and survival of rosette-derived neuron types in vivo are unique to the rosette stage and not observed in NSC$^{FGF2/EGF}$. Therefore, rosette stage cells are referred to as "R-NSCs" for the remainder of this study.

Genetic characterization of R-NSCs and NSCs$^{FGF2/EGF}$

Global gene expression analysis in R-NSCs confirmed anterior bias in Forse1$^+$ versus Forse1$^-$ R-NSC progeny (Fig. 4A). Forse1$^+$ R-NSCs were also enriched in markers associated with NSC fate. However, a few NSC markers were enriched in the Forse1$^-$ compartment, including

ID1 and Hes5, suggesting regional differences in NSC marker expression along the AP axis. Forse1$^-$ cells were enriched for caudal CNS markers and markers of differentiating neuroblasts. The most notable enrichment within the Forse1$^-$ compartment concerned the expression of markers indicative of neural crest fate (Fig. 4A). Neural crest identity was corroborated by enrichment for the neural crest precursor marker p75 after FACS-mediated isolation of Forse1$^-$ cells in vitro (data not shown) and after transplantation of Forse1$^-$ R-NSCs in vivo (Supplemental Fig. 8). While Forse1$^+$ cells were negative for neural crest markers, neural crest differentiation could be induced after RA-mediated caudalization (data not shown). These data demonstrate that Forse1$^+$ R-NSCs are biased toward anterior fates but retain the capacity to generate caudal fates. Forse1$^-$ R-NSCs are enriched in posterior CNS markers and exhibit increased potential for both neural crest differentiation and specification toward caudal CNS neuron fates.

R-NSCs and NSCs$^{FGF2/EGF}$ share expression of key NSC markers but are distinct in differentiation potential. We next attempted the identification of genes unique to the R-NSC stage by comparing global gene expression profiles of Forse1$^+$ and Forse1$^-$ R-NSCs versus Forse1$^+$ NSCs$^{FGF2/EGF}$. Forse1$^-$ NSCs$^{FGF2/EGF}$ were excluded from the analysis as Forse1$^+$ NSCs$^{FGF2/EGF}$ were enriched for NSC features compared with Forse1$^-$ NSCs$^{FGF2/EGF}$. A Venn diagram was established comparing transcripts significantly increased in any of the three NSC populations compared with undifferentiated hESCs. A total of 2389 transcripts were identified with expression levels five times or higher compared with undifferentiated hESCs (Fig. 4B). Since Forse1$^+$ and Forse1$^-$ population are distinct but both share R-NSC properties, we hypothesized that R-NSC-specific genes are shared between Forse1$^+$ and Forse1$^-$ R-NSCs but are not expressed in either NSCs$^{FGF2/EGF}$ or undifferentiated hESCs. This analysis revealed 298 R-NSC-specific genes (Fig. 4B). Genes with the highest levels of differential expression included many transcription factors such as PLAGL1, Dach1, and PLZF (ZBTB16). The group of 449 genes shared among all three NSC populations included most of the known NSC markers including FABP7 and SOX1. The top marker was Zic1, a gene not previously associated with NSC identity but reported to be expressed in neuroectodermal precursors during mouse development (Nagai et al. 1997) and early neural progeny derived from hESCs (Pankratz et al. 2007). Markers specific to NSC$^{FGF2/EGF}$ stage comprised a total of 1209 transcripts including later stage neural precursor markers such as S100B and AQP4 (Fig. 4C). All gene expression data are deposited in public databases (Gene Expression Omnibus (GEO): accession no. GSE9921.

Immunocytochemical analysis was used to confirm specificity of key R-NSC, shared R-NSC/NSC$^{FGF2/EGF}$ and NSC$^{FGF2/EGF}$ markers in vitro (Fig. 4D,E; Supple-

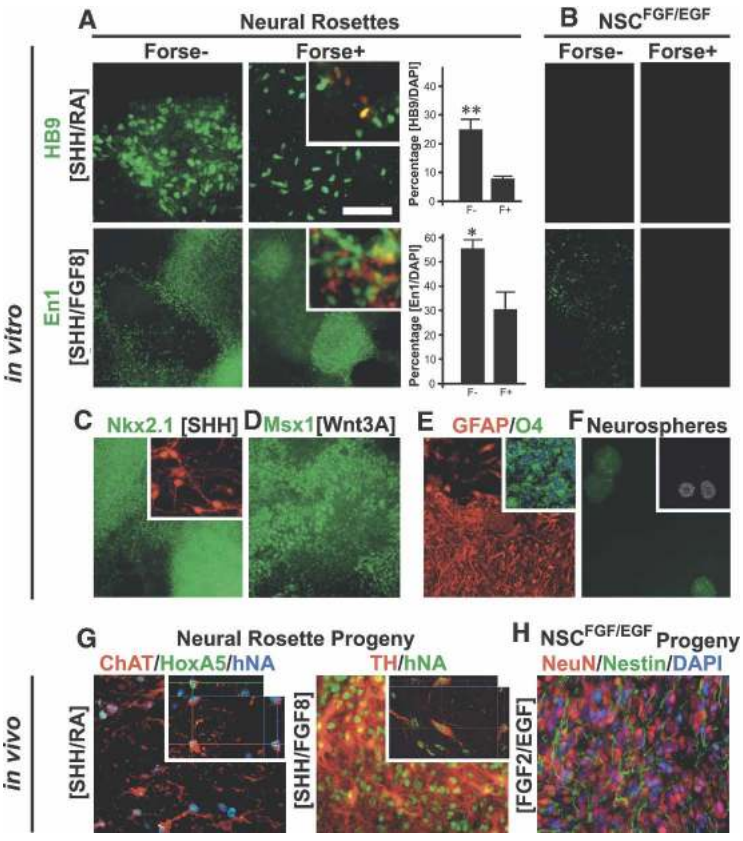

Figure 3. Respecification of anterior neural rosettes toward caudal fates. (*A*) Analysis and quantification of HB9$^+$ motoneurons and En1$^+$ midbrain precursors in response to SHH/RA- or SHH/FGF8-mediated patterning, respectively, of Forse1$^+$ and Forse1$^-$ rosette stage cells. *Insets* show representative images following clonal analyses for GFP$^+$ Forse1$^+$ rosette stage cells exposed to SHH/RA or SHH/FGF8, respectively. *Top inset*) HB9 (red) and GFP (green). (*Bottom inset*) En1 (red) and GFP (green). Statistical analysis: mean ± SEM; (**) $P < 0.01$; (*) $P < 0.05$; ANOVA. (*B*) Results for SHH/RA- or SHH/FGF8-treated Forse1$^+$ and Forse1$^-$ NSCs$^{FGF2/EGF}$ showing a complete lack of HB9$^+$ motoneurons and near complete lack of En1$^+$ precursors. (*C*) Immunocytochemistry for the ventral forebrain marker Nkx2.1 upon exposure of Forse1$^+$ rosette stage cells to SHH. (*Inset*) Prolonged differentiation yielded cells immunoreactive for GABA (red). (*D*) Induction of the dorsal marker Msx1 was observed upon exposure of Forse1$^+$ rosette stage cells to Wnt3A. (*E*) Analysis for GFAP and O4 (*inset*) expression in rosette stage cells expanded in FGF2/EGF followed by exposure to CNTF or T3, respectively. (*F*) Neurosphere formation of Forse1$^+$ R-NSCs and Forse1$^-$ R-NSCs (*inset*; note differences in size). (*G*) In vivo survival of spinal motoneurons and midbrain dopamine neurons derived from rosettes in vitro. *Insets* show confocal image stacks after 3D reconstruction confirming human identity of the grafted cells. (*H*) Expression of neuronal markers in NSC$^{FGF2/EGF}$ progeny in vivo. Bar in *A*, (*top right* panel) corresponds to 100 µm in *A* and *B* (*top* panels), and *D*, *E*, *G*, and *H*; 200 µm in *C*; 250 µm in *A* and *B* (*bottom* panels); and 500 µm in *F*.

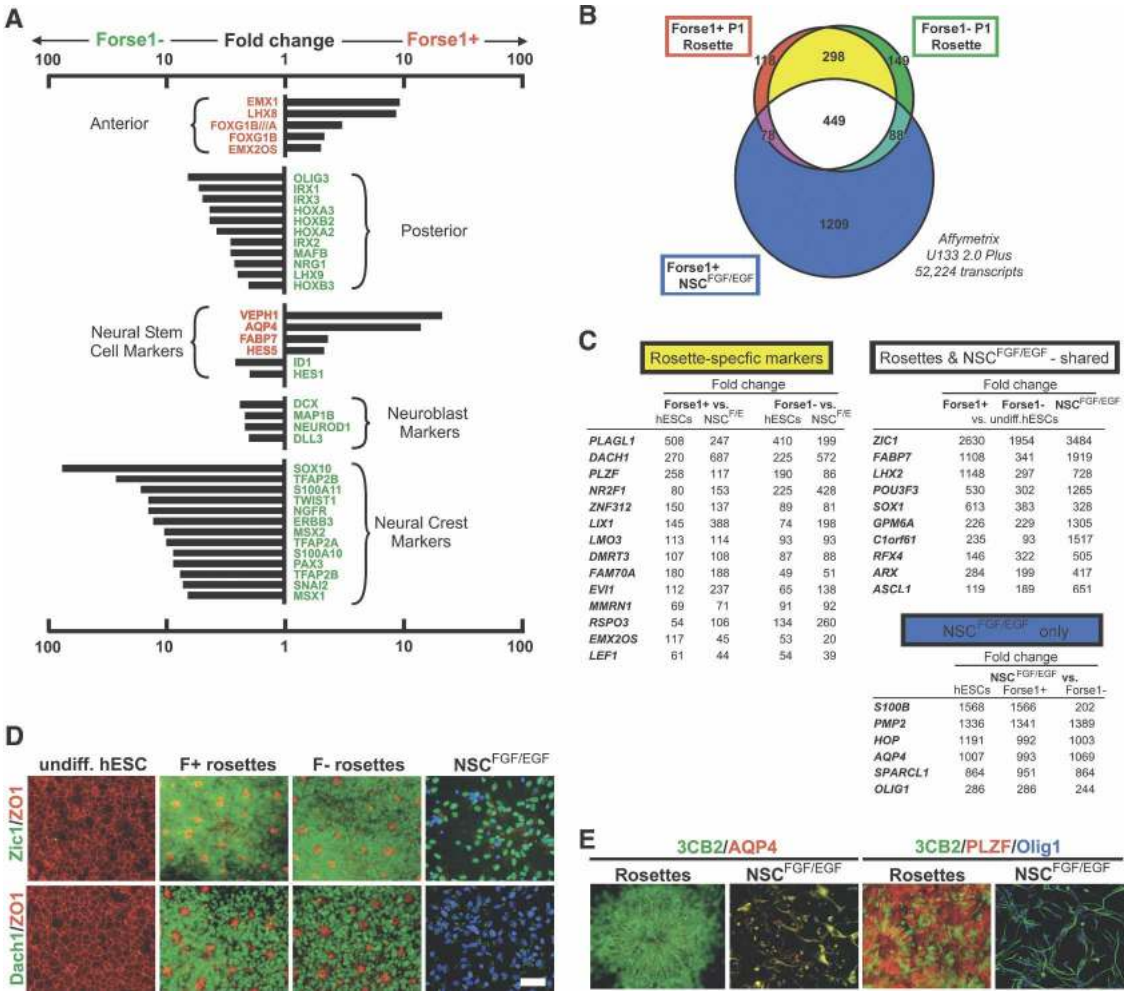

Figure 4. Genetic characterization of R-NSCs and NSCs$^{FGF2/EGF}$. (*A*) Global gene expression analysis (Affymetrix, U133-Plus2) comparing Forse1^{+} versus Forse1^{-} R-NSCs at P1 (day 25). (*B*) Venn diagram representing genes specifically expressed in Forse1^{+} (red) and Forse1^{-} (green) R-NSCs, and in Forse1^{+} NSCs$^{FGF2/EGF}$ (blue). R-NSC-specific genes are marked in yellow, while genes shared between all three NSC groups are marked in white. (*C*) Fold changes calculated from Affymetrix analysis for the top differentially expressed transcripts. Fold changes are grouped into those specific for R-NSCs, those shared between R-NSCs and NSCs$^{FGF2/EGF}$, and those specific to NSCs$^{FGF2/EGF}$. (*D*) Immunocytochemical confirmation of representative markers shared between R-NSCs and NSCs$^{FGF2/EGF}$ (Zic1), or markers specific to R-NSC state (Dach1). (*E*) Colabeling studies of 3CB2 and NSCs$^{FGF2/EGF}$-specific (AQP4) or R-NSC-specific (PLZF) markers. Bar in *D* corresponds to 50 μm for all panels.

mental Fig. 9). Quantification and specificity of all key R-NSC markers was validated and confirmed by quantitative RT–PCR (qRT–PCR) analysis (Supplemental Fig. 10). R-NSC marker expression was not limited to in vitro culture, as expression was maintained in R-NSC progeny in vivo 4 wk after transplantation into the adult rat striatum. Grafted NSCs$^{FGF2/EGF}$ lacked expression of R-NSC markers in agreement with in vitro data. Sets of transplanted R-NSCs also retained rosette cytoarchitecture, as illustrated by ZO-1^{+} lumens and distribution of M-phase cells indicative of interkinetic nuclear migration (Supplemental Fig. 11). Enrichment of neural crest progeny in Forse1^{-} rosette stage cells was confirmed in vivo upon transplantation of Forse1^{-} P1 cells into the adult rat striatum (Supplemental Fig. 8).

Notch and SHH signaling are required for R-NSC maintenance

We next set out to develop culture conditions for the in vitro expansion of R-NSCs. We first investigated the effect of cell density on rosette maintenance. Dissociated P2 R-NSCs maintained in the presence of SHH/FGF8 efficiently reformed rosettes with a near absence of neuronal differentiation, if plated at high cell densities. In contrast, low plating densities resulted in increased levels of neuronal differentiation and a significant reduction in rosette formation efficiency (Fig. 5A). These data suggest that endogenous density-dependent signals are critical for maintaining R-NSC state. Notch is a signaling pathway that has been implicated in stem cell maintenance and cell-to-cell signaling (Artavanis-Tsakonas et

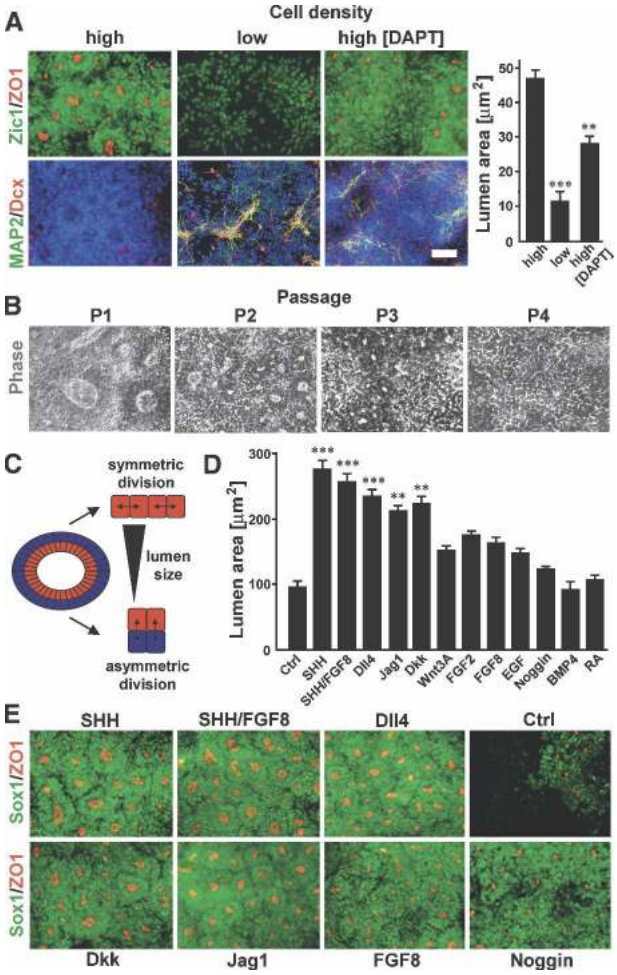

Figure 5. Effects of cell density, SHH, and Notch signaling pathways on R-NSC maintenance. (*A*) Effect of cell plating density and DAPT treatment on rosette reformation (Zic/ZO-1) and spontaneous neuronal differentiation (MAP2/Dcx) in dissociated P2 R-NSCs. *Right* panel shows quantification of rosette lumens as a surrogate marker of rosette growth. Statistical analysis: mean ± SEM; (***) $P < 0.001$; (**) $P < 0.01$ (compared with high density; ANOVA: Newman-Keuls test). (*B*) Phase contrast images of R-NSCs maintained in SHH/FGF8 over multiple passages (loss of rosette structure). (*C*) Schematic model illustrating symmetric versus asymmetric division mode in rosettes and relationship to lumen size. (*D*) Quantification of ZO-1$^+$ rosette lumen size in P2 R-NSC cultures treated with various agonists and antagonists of candidate signaling pathways. Statistical analysis: mean ± SEM; (***) $P < 0.001$; (**) $P < 0.01$ (compared with control; ANOVA: Dunnett test). (*E*) Representative images (ZO-1/Sox1) of P2 R-NSC cultures at day 4 of treatment with candidate factors. Scale bar in *A* corresponds to 50 μm in *A* and *B*, and 75 μm in *E*.

al. 1999). Exposure of high-density R-NSCs to DAPT, a pharmacological inhibitor of the Notch pathway, was sufficient to induce premature neuronal differentiation and to significantly disrupt rosette morphology (Fig. 5A). Continued growth and passage of R-NSCs at high cell densities resulted in spontaneous differentiation and loss of rosette morphology (Fig. 5B). Therefore, we designed a candidate screen aimed at the identification of signaling molecules that permit long-term R-NSC expansion. The screening strategy was based on measuring rosette lumen size as used for the quantification of rosette formation in Figure 5A. This measure is based on the assumption that rosettes expand in size through symmetric division, reflected by an increase in the size of the rosette lumen over time. On the other hand, asymmetric division of R-NSC progeny, such as neuronal differentiation and/or migration outside of rosettes, will lead to a decrease in lumen size (Fig. 5C). We found that treatment with Notch and SHH agonists induced the most robust increases in lumen size and overall rosette growth (Fig. 5D,E). A significant increase in lumen size was also observed upon treatment with Dkk, suggesting an involvement of Wnt signaling in the control of rosette maintenance.

We next tested whether the combination of SHH and Notch agonists is sufficient for long-term R-NSC maintenance. High-density P2 R-NSCs were replated in the presence of FGF2/EGF, SHH/FGF8, SHH/Dll4/Jag, or SHH/Dll4/Jag/FGF8. At P3, rosette morphology was maintained under all conditions (Fig. 6A) except FGF2/EGF treatment, which led to a rapid loss of rosette morphology (data not shown). In contrast, at P4 only SHH/Dll4/Jag treatment was sufficient to retain rosette structure in R-NSC cultures (Fig. 6A). Addition of FGF8 to SHH/Dll4/Jag resulted in the loss of rosette morphology, suggesting that long-term exposure to FGF8 can override the effects of the SHH and Notch pathways on rosette maintenance. Conditions best at maintaining rosette morphology were also superior in R-NSC proliferation (Fig. 6B). Immunocytochemical analysis (Fig. 6C) confirmed maintenance of both rosette morphology (ZO-1) and R-NSC marker expression (PLZF) in the presence of SHH/Dll4/Jag. R-NSC progeny cultured in the presence of FGF2/EGF or SHH/FGF8 showed a loss of rosette morphology, a decrease in R-NSC markers, and a concomitant increase of markers associated with NSCs$^{FGF2/EGF}$ such as S100B. Generic NSC markers shared between R-NSCs and NSCs$^{FGF2/EGF}$ such as Zic1 and 3CB2 were maintained under all treatment conditions. We next assessed the lineage relationship of R-NSCs and NSCs$^{FGF/EGF}$ at the clonal level. To this end Forse1$^+$/N-cad^{high} rosette stage cells were isolated from RU-01eGFP and replated at single-cell density on stage-matched high-cell-density rosette cells from H9 (WA-09) in the presence of SHH/FGF8. These data showed loss of PLZF expression in a subset of clonally derived R-NSC progeny with a concomitant loss of rosette morphology and increased expression of the NSCs$^{FGF2/EGF}$ marker S100B (Fig. 6D).

In addition to analyzing individual R-NSC markers, we established an algorithm termed "rosette score" to read out gene expression for the full set of 298 R-NSC markers (Fig. 6E; see Materials and Methods for details). As expected, NSCs$^{FGF2/EGF}$ showed a dramatic decrease in rosette score. In contrast, P2 R-NSCs exhibited a slight increase in rosette score compared with P1 R-NSCs, suggesting enrichment of either R-NSC purity

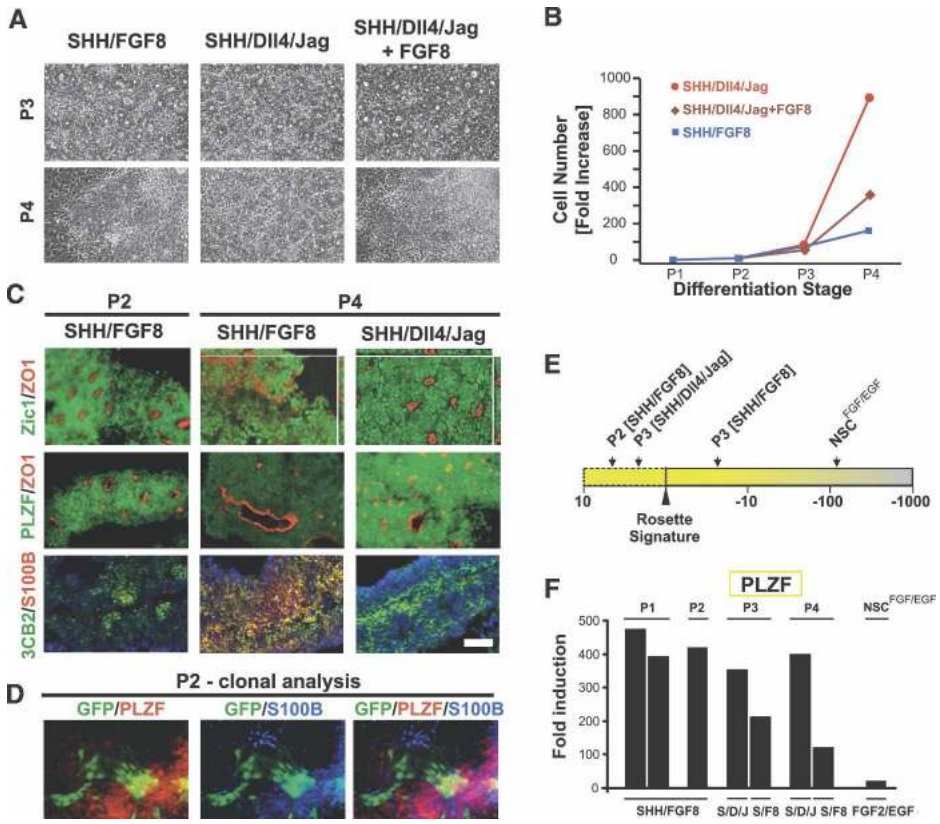

Figure 6. R-NSC maintenance and transition to NSCs$^{FGF2/EGF}$ stage. Representative phase-contrast images (*A*) and growth curves (*B*) over multiple passages in R-NSC cultures maintained with candidate growth factor regimens. (*C*) Corresponding immunocytochemical analyses for rosette structure (Zic1/ZO-1), markers of R-NSCs (PLZF), NSCs$^{FGF2/EGF}$ (S100B), and radial glia (3CB2). (*D*) Clonal analysis of constitutively eGFP-expressing R-NSCs sorted for Forse1. Cells are shown at the transition toward NSCs$^{FGF/EGF}$ with partial loss of PLZF expression and loss of epithelial organization in a subset of clonally derived eGFP$^+$ cells. (*E*) Effect of passage and growth regimen on "rosette score," a composite measure for gene expression for all 298 R-NSC markers. (*F*) qRT–PCR analysis for PLZF expression over passage in SHH/Dll4/Jag- versus SHH/FGF8-treated R-NSCs. Bar in *C* corresponds to 50 µm in *A* and *C*.

or marker expression. Importantly, at P3 we observed a clear difference in rosette scores between R-NSCs treated with SHH/FGF8 (negative score) versus those maintained in SHH/Dll4/Jag (positive score) (Fig. 6E). qRT–PCR analysis for PLZF, a key R-NSC marker, confirmed loss of expression in SHH/FGF8 treated R-NSCs versus those maintained in SHH/Dll4/Jag at P3. The difference between the two treatment conditions continued to increase at P4 (Fig. 6F).

R-NSCs exhibit in vivo overgrowth

While transplantation of undifferentiated hESCs leads to teratomas, the transplantation of NSC$^{FGF2/EGF}$ into the adult rodent brain results in long-term graft survival and neural stem-like behavior in the host striatum and SVZ (Tabar et al. 2005). Here we tested the in vivo growth behavior of cultures at the R-NSC stage. Histological analysis of P2 R-NSC grafts 4 wk after transplantation (Fig. 7A) revealed signs of neural overgrowth, as evidenced by large grafts composed of rosette structures maintaining Pax6 expression. Rosettes were surrounded by a zone of differentiating neurons. Rosette formation and overgrowth behavior was retained after FACS-mediated isolation of Forse1$^+$ R-NSCs, supporting the hypothesis that in vivo growth is caused by R-NSCs rather than a rare population of contaminating undifferentiated hESCs. However, to rule out the possibility of ESC contribution completely, future studies should test in vivo growth potential in R-NSCs derived from primary CNS tissue (see below). Interestingly, neural overgrowth directly from primary CNS tissue has been reported in the past upon transplantation of human basal forebrain precursor into rodent models of Huntington's disease (Geny et al. 1994). The propensity for continued rosette growth in vivo may have important implications in the context of recent studies reporting signs of neural overgrowth and spontaneous forebrain fates in vivo upon transplantation of ESC-derived dopamine neurons in rodent models of PD (Ferrari et al. 2006; Roy et al. 2006). Understanding rosette biology will be critical for harnessing in vitro differentiation potential and controlling in vivo growth behavior.

R-NSCs can be derived from mouse ESCs and primary neural plate cultures

The functional genetic characterization of R-NSCs will be significantly accelerated through the availability of

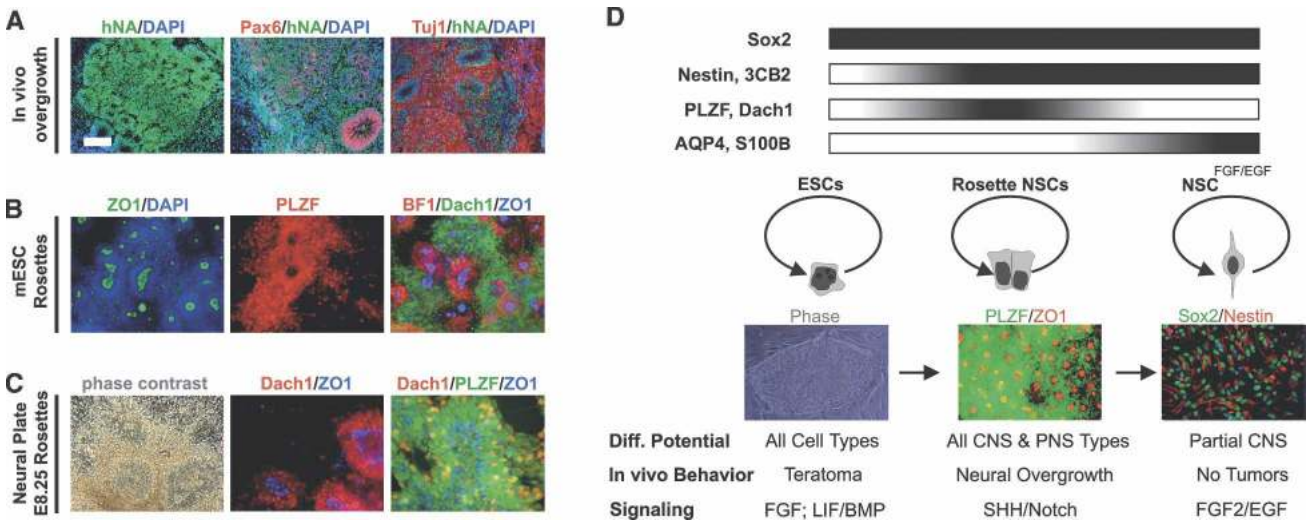

Figure 7. Generalization of neural rosette biology: in vivo maintenance, derivation from mouse ESCs and from primary neural plate tissue. (*A*) In vivo behavior of hESC-derived rosettes: immunohistochemical analysis of R-NSC progeny 4 wk after transplantation into the adult rat striatum. (*B*) Characterization of mouse ESC-derived neural rosettes: Immunocytochemical analysis is shown for rosette structure (ZO-1,DAPI), R-NSC marker (PLZF, Dach1), and anterior fate (BF1). (*C*) Neural rosettes derived from primary mouse neural plate: Anterior neural plate tissue from E8.25 mouse embryos was maintained for 4 d in the presence of SHH/Dll4/Jag. Emerging rosettes were characterized for rosette structure (phase-contrast image, ZO-1) and R-NSC marker expression (Dach1, PLZF). Bar in *A* corresponds to 50 µm in *C* (*middle* and *right* panels); 100 µm in *A* (*middle* and *right* panels), *B* (all panels), and *C* (*left* panel); and 150 µm in *A* (*left* panel). (*D*) Model of neural rosette biology: R-NSCs are proposed to represent a novel NSC stage intermediate between undifferentiated ESCs and FGF2/EGF-expanded NSCs ($NSCs^{FGF2/EGF}$) with distinct marker expression, morphology, fate potential, in vivo behavior, and signaling requirements (see the text for details).

protocols suitable for the isolation of mouse ESC-derived rosettes. To this end we adapted a recently established SFEB protocol (Watanabe et al. 2005) for R-NSC derivation (Fig. 7B). At day 5 of differentiation SFEBs were dissociated into single cells and replated at high density (P1 stage) in the presence of factors shown to promote rosette maintenance from hESCs. Under high-density culture conditions SFEB progeny yielded R-NSCs expressing PLZF and exhibiting ZO-1^+ rosette lumens. The majority of mouse ESC-derived R-NSCs expressed BF1 suggesting anterior CNS bias similar to R-NSCs derived from hESCs. Other rosette markers such as Dach1 were also observed in mouse ESC-derived R-NSCs.

We next attempted the isolation of R-NSCs directly from primary CNS tissue. To that end E8.25 anterior neural plate tissue was isolated, dissected, and mechanically dispersed into small colonies grown in the presence of SHH/Dll/Jag. After 24–48 h of in vitro culture, the formation of $PLZF^+$ and $Dach1^+$ rosette structures was visible, centered around ZO-1^+ lumens (Fig. 7C). Under the conditions tested, efficient derivation of R-NSC like structures from primary mouse tissue appeared restricted to the stages prior to E9.5 with a dramatic drop in the efficiency of R-NSC derivation at later developmental stages. Our data in mouse ESCs and primary neural tissue suggest that cells with R-NSC properties exist at the neural plate stage, and that such cells may represent the earliest NSC stage in vivo.

Discussion

Our work demonstrates that R-NSCs represent a novel stem cell state in the progression of ESCs toward differentiated neural fates as summarized in Figure 7D. While R-NSCs share markers with both ESCs and $NSCs^{FGF2/EGF}$ including Sox2, markers such as PLZF and Dach1 are specific to R-NSC state. The progression of R-NSCs to $NSCs^{FGF2/EGF}$ is reflected by the induction of $NSCs^{FGF2/EGF}$-specific markers such as S100B and AQP4. Classic markers of NSC fate are shared between R-NSCs and $NSCs^{FGF2/EGF}$. This indicates that NSCs properties emerge at the R-NSC stage but that R-NSCs inevitably progress toward the $NSCs^{FGF2/EGF}$ stage under standard NSC growth conditions. One of the most important properties of R-NSCs is their comprehensive differentiation potential toward CNS and PNS fates. Given the limited potential of $NSCs^{FGF2/EGF}$ to yield early type projection neurons, such as spinal motoneurons or midbrain dopamine neurons, R-NSCs may represent the first NSC type capable of recreating the full neuronal diversity. However, broad differentiation potential is accompanied with extensive growth potential as reflected by neural overgrowth observed upon transplantation of R-NSCs into the adult CNS. Similar to undifferentiated ESCs that pose a risk for teratoma formation, R-NSCs will require techniques that harness differentiation potential while addressing the risk for neural overgrowth in vivo. The unique signaling required for maintaining R-NSCs will guide efforts aimed at eliminating R-NSCs at the time of transplantation. Obvious strategies include treatment with antagonists of Notch and SHH signaling that promote neuronal differentiation of R-NSCs. Treatment with FGF2/EGF will induce transition of R-NSCs to $NSCs^{FGF2/EGF}$ that have a low risk of tumor formation but exhibit more restricted differentiation potential. Spe-

cific neuron types derived from R-NSC cultures such as spinal motoneurons or midbrain dopamine neurons retain post-mitotic status and phenotypic properties upon transplantation. This suggests that understanding the molecular control of R-NSC maintenance versus differentiation will be critical in developing cell-based strategies in neurodegenerative disease.

The prospective isolation of Forse1$^+$/N-cad$^+$ R-NSCs enabled us to demonstrate respecification of anterior BF1$^+$ neuroectodermal cells toward caudal fates including spinal motoneurons and midbrain dopamine neurons. Forse1 could become a powerful tool to isolate NSC populations with anterior CNS bias at various stages of development to probe developmental competency. Default acquisition of anterior neural fate observed in R-NSCs is reminiscent of the anterior neural default model postulated in classical studies of *Xenopus* CNS development. These studies showed that anterior CNS fates are established first and are followed by caudal transformation in response to secreted signals (for review, see Sasai and De Robertis 1997). Forse1$^-$/N-cad$^+$ R-NSCs correspond to posterior regions of the neuroepithelium with the capacity to generate neural crest lineages. Neural crest differentiation potential reflects the early developmental stage and broad differentiation potential of R-NSCs, as neural crest specification in vivo occurs at the neural plate stage (Yamada et al. 1993; LaBonne and Bronner-Fraser 1999). The isolation of Forse1$^-$ R-NSCs provides a novel strategy for studying early human neural crest development in vitro. Neural crest potential of R-NSCs also points to the importance of monitoring neural crest fates in studies aimed at the generation of defined CNS derivatives. Forse1$^+$ cells lack neural crest markers but retain the plasticity toward neural crest fates upon exposure to caudalizing cues that suppress anterior CNS identity.

While R-NSCs and NSCs$^{FGF2/EGF}$ share expression of common NSC markers including Nestin, Sox2, 3CB2, our data define a set of unique R-NSC-specific molecular markers. It is tempting to speculate that the great number of transcription factors such as zinc-finger and homeodomain proteins, enriched in the R-NSC stage, may have a functional role in R-NSC induction and maintenance. One such candidate factor is PLZF, a zinc-finger protein involved in self-renewal of adult male germ stem cells (Buaas et al. 2004; Costoya et al. 2004) and highly expressed in multipotent hematopoietic precursors (Reid et al. 1995). PLZF is known to bind the polycomb group protein BMI-1, a crucial component in hematopoietic and NSC self-renewal. In the nervous system, PLZF is expressed broadly at the neural plate-stage followed by a temporally dynamic spatial restriction to rhombomere boundaries followed by rapid loss of expression by day 10.5 of mouse development (Cook et al. 1995). PLZF expression has also been reported in RA-treated P19 embryonal carcinoma cells at early stages of neural differentiation (Cook et al. 1995). These reports are compatible with a possible role for PLZF in rosette maintenance and with the model that neural rosettes represent an early neural plate-like stage of development. PLZF and Evi-1, another highly expressed R-NSC marker, are also known factors associated with acute myelogenic leukemias (Morishita et al. 1992; Grignani et al. 1998). Evi-1 acts as a repressor of TGF-β signaling via inhibition of SMAD3 (Kurokawa et al. 1998). Interestingly, Dach1 can also participate in negative regulation of TGF-β signaling via interaction with NCoR and Smad4 (Wu et al. 2003), suggesting that repression of TGF-β signaling may be critical for rosette maintenance.

Our study provides multiple evidence for the involvement of Notch signaling in rosette maintenance, including DAPT-mediated induction of neuronal differentiation in R-NSCs as well as enhanced maintenance of R-NSC state and proliferation in the presence of Dll4 and Jag1. Notch is a well-known regulator of NSC self-renewal in the developing and adult CNS (Artavanis-Tsakonas et al. 1999). Data from studies in NSCs suggest increased levels of symmetric divisions (Shen et al. 2004) and reduced cell death (Androutsellis-Theotokis et al. 2006) upon Notch activation. Genetic evidence in mouse development suggests that Notch1 signaling promotes radial glia identity (Gaiano et al. 2000). Another set of recent studies in mice has shown that loss of function of the Lgl1 gene (Lethal giant larvae 1) induces neural rosette formation in vivo by preventing asymmetric localization of the Notch inhibitor Numb (Klezovitch et al. 2004). The effect of SHH on R-NSC growth and maintenance could be due to general effects on cell proliferation. SHH is a well-known mediator of cell proliferation for cerebellar granule cell precursors (Wechsler-Reya and Scott 1999) and precursors of the developing and adult forebrain (Machold et al. 2003). SHH has also been shown to regulate cell proliferation and survival in early neuroepithelial precursors, prior to E9.0 (Ishibashi and McMahon 2002), a stage that most closely mimics the stage represented in R-NSCs. Other possible mechanisms of SHH action on R-NSC growth include SHH-mediated ventralization (Roelink et al. 1995) and suppression of dorsal CNS fates (Yamada et al. 1993), including neural crest lineages, associated with loss of rosette structure. SHH could also act indirectly via activation of Notch signaling, as shown in cerebellar granule cell proliferation (Solecki et al. 2001). Finally, activation of the SHH pathway in mouse models causes epithelial tumors such as basal cell carcinoma and medulloblastoma (Goodrich et al. 1997). Rosette formation is one of the key histopathological features of human medulloblastomas. Future studies are required to further explore the effect of Wnt signaling on rosette growth. The effect of Dkk on rosette growth and the dramatic enrichment of LEF1 mRNA in R-NSCs versus NSCs$^{FGF/EGF}$ suggest that Wnt signals may affect rosette biology in a complex manner.

In early development, neural precursors transit from nestin$^+$ single-layer neurepithelial cells into FABP7$^+$ radial glial cells that progress to a S100B$^+$ stage and eventually give rise to GFAP-expressing adult NSCs (Gotz and Barde 2005). Recent studies have reported the generation of ESC-derived precursor cells with radial glia properties (Bibel et al. 2004) that can be propagated in the presence of FGF2/EGF (Conti et al. 2005). In our study

R-NSCs indeed express markers of radial glia, and these markers are maintained after FGF2/EGF expansion ($NSC^{FGF2/EGF}$ stage). However, FGF2/EGF expanded R-NSCs showed a dramatic increase in $NSC^{FGF2/EGF}$ markers such as S100B and loss of rosette markers. While radial glia identity is considered a hallmark of NSC identity (Alvarez Buylla et al. 2001), our data show clear differences in competency of R-NSCs versus $NSC^{FGF2/EGF}$ cultures. Our data suggest that R-NSCs can be converted at the clonal level into cells expressing $NSC^{FGF2/EGF}$ markers. However, we cannot exclude the possibility that some $NSCs^{FGF2/EGF}$ could also be generated without going through an obligate R-NSC intermediate. Future studies should also address whether epithelial organization is functionally important for maintaining R-NSC properties and whether disruption of this organization is critical in $NSCs^{FGF2/EGF}$ transition. Location of M-phase cells adjacent to ZO-1^+ rosette lumens indicates that the lumen may act as a niche regulating rosette growth. Mechanisms that may require rosette structure, and the presence of a luminal niche include control of symmetric versus asymmetric cell division and competency to respond to spatial patterning cues.

Our work demonstrates conditions that direct R-NSCs toward one of the following stages: maintenance of rosette state (high density, SHH/Dll/Jag), transition to $NSC^{FGF2/EGF}$ (FGF2/EGF), or neuronal differentiation (low density/DAPT). The isolation of R-NSCs as a novel more universal NSC stage has important implications for both basic NSC biology and for applications in regenerative medicine. The list of R-NSC-specific transcripts should yield an extensive set of markers for the prospective isolation and characterization of neural rosettes. It should also shed light onto the transcriptional networks regulating R-NSC function. Another fundamental question in rosette biology concerns the existence of an in vivo correlate of R-NSCs during neural development and whether similar cells persist in the adult CNS. While our data indicate that rosettes most closely mimic the neural plate stage, the availability of defined R-NSC markers will be a starting point to probe the presence of R-NSCs at later developmental stages. Finally, it will be critical to test whether R-NSC-specific transcription factors can induce R-NSC features in $NSCs^{FGF2/EGF}$. The feasibility of reprogramming cells from more accessible NSC stages would have important implications in regenerative medicine. While exposure of $NSCs^{FGF2/EGF}$ to SHH/Dll/Jag seems not sufficient to induce conversion to R-NSC state (data not shown) overexpression of key R-NSC transcription factors may be a promising complementary strategy toward this end.

The NSC progression model proposed here is compatible with changes in competency observed in other stem cell types. Both developmental and region-specific bias in differentiation potential has been reported in neural crest stem cells (Bixby et al. 2002; Kruger et al. 2002). In mesenchymal stem cells early precursors derived from hESCs efficiently yield skeletal muscle fates (Barberi et al. 2007), a fate not readily accessible to adult mesenchymal stem cells (Pittenger et al. 1999).

In conclusion, we demonstrated the isolation and the genetic and functional characterization of a novel more universal NSC stage. Our findings should facilitate studies of early human neural development and significantly improve our ability to use NSC derivatives in regenerative medicine. The broad differentiation potential of R-NSCs suggests that these cells may represent the first neural cell type that—similar to stem cells in the hematopoietic system—is capable of generating the full cellular diversity in the mammalian nervous system.

Materials and methods

Culturing undifferentiated hESCs

hESC lines H9 (WA-09, XX, P25–35), H1 (WA-01, XY, P30–50), and RU-01eGFP (James et al. 2006) (XY, P15–30) were cultured on mitotically inactivated mours embryonic fibroblasts (MEFs) (Specialty Media). Undifferentiated hESCs were maintained as described previously (Zhang et al. 2001; Perrier et al. 2004).

Neural induction and rosette formation

MS5 stromal cells were grown in a-MEM medium containing 10% FBS and 2 mM L-glutamine (Barberi et al. 2003). Neural differentiation of hESCs was performed as described previously (Perrier et al. 2004). Feeder-free neural induction and rosette formation were based on an EB-based approach (Zhang et al. 2001), although we extended the EB stage from 4 d to 6–10 d.

Rosettes were harvested mechanically, beginning on day 14 of differentiation (MS5 system) or day 6 after replating (EB system, day 12–16 of differentiation). Rosettes were replated on culture dishes precoated with 15 µg/mL polyornithine/1 µg/mL laminin (Po/Lam) in N2 medium supplemented with SHH (200 ng/mL), FGF8 (100 ng/mL), ascorbic acid (AA, 0.2 mM), and BDNF (20 ng/mL). Replated rosettes were defined as P1 R-NSC cultures. After 7–9 d (80% confluency), cells were dissociated after incubation (1 h) in Ca^2/Mg^2-free HBSS. Cells were resuspended and plated onto Po/Lam culture dishes. For R-NSC maintenance, cells were seeded at 400×10^3 cells per square centimeter in the presence of AA/BDNF and/or SHH (500 ng/mL), FGF8 (100 ng/mL), Dll4 (500 ng/mL), Jagged-1 (Jag; 500 ng/mL), FGF2 (20 ng/mL), and EGF (20 ng/mL) (all from R&D Systems). For neural patterning, R-NSCs were seeded at 50×10^3 per square centimeter in the presence of AA/BDNF and were exposed to SHH (200 ng/mL) and RA (1 µM) for 12 d (spinal motoneurons), or SHH (200 ng/mL) and FGF8 (100 ng/mL) for 8 d (midbrain precursors). Other conditions tested for R-NSC maintenance/differentiation include Dkk (100 ng/mL), Wnt3A (40 ng/mL), Noggin (500 ng/mL), and BMP4 (50 ng/mL) (all R&D Systems); DAPT (5 µM; Calbiochem); and Cyclopamine (1 µM; Sigma). For clonal density assays, see the main text and Supplemental Material.

Immunocytochemistry and RT–PCR analyses

Fixation in 4% paraformaldehyde/0.15% picric acid was followed by immunocytochemical analysis. A complete list of antibodies and conditions is provided in the Supplemental Material. RT–PCR analyses were performed after RNA extraction (RNeasy), DNase I treatment (Qiagen), and reverse transcription (SuperScript, Invitrogen). Linear amplification range was determined for each primer. PCR products were identified by size, and identity was confirmed by DNA sequencing. MS5 cells were negative for all primers used in this study. When cocul-

tured with MS5, hESC progeny was mechanically separated from feeders to avoid cross-contamination. Primer sequences, cycle numbers, and annealing temperatures are provided upon request.

For qRT–PCR analysis, 20 ng of cDNA per sample were used on an iCycler (Bio-Rad) with predesigned TaqMan Probes for PLAGL1, ZNF312, PLZF, LEF1, NR2F1, DMRT3, LMO3, S100B, and HPRT. Threshold cycle values were determined in triplicate and presented as average normalized to HPRT. Fold changes were calculated using the $2^{-\Delta CT}$ method.

FACS

Cells were dissociated with Accutase (Innovative Cell Technologies, Inc.) and subjected to FACS using SSEA4 (1:75; DSHB), Forse1 (1:75; DSHB), or N-Cadherin (1:100; Sigma) antibodies on a MoFlo flow cytometer (Cytomation).

Gobal gene expression analysis

For identification of R-NSC-specific transcripts, RNA (200 ng) was obtained from SSEA4$^+$ hESCs, P1 R-NSCs (sorted for Forse1$^-$/N-Cad^{high} or Forse1$^-$/N-Cad^{high}), and NSCs$^{FGF2/EGF}$ (sorted for Forse1$^+$/N-Cad$^+$). For the R-NSC maintenance assay, samples were obtained from P2 and P3 R-NSCs maintained in SHH/FGF8, and P3 R-NSCs maintained in SHH/Dll4/Jag. All samples were processed by the MSKCC Genomics Core Facility and hybridized on Affymetrix U133-Plus2 human oligonucleotide arrays. Fold changes and significance values for the direct comparison of Forse1$^+$/N-Cad^{high} versus Forse1$^-$/N-Cad^{high} cells were calculated using GCOS (Affymetrix). Venn diagram was established using previously published statistical criteria (Barberi et al. 2007). A detailed description is provided in the Supplemental Material.

Maintenance of R-NSC marker profile under various treatment regimens was estimated by calculating the effective distance ("rosette score") of each treatment condition on a vector between the P1 R-NSC and NSC$^{FGF2/EGF}$ state. Negative or positive distance values indicate loss or increase in rosette markers, respectively. Detailed information and a mathematical description of the procedure are in the Supplemental Material.

All microarray data are available on GEO (accession no. GSE9921).

Animal surgery and isolation of neural plate

All animal experiments were done in accordance with protocols approved by our Institutional Animal Care and Use Committee and following NIH guidelines for animal welfare. Stereotactic implantations were performed into the striatum (Tabar et al. 2005) (100,000 NSCs$^{FGF/EGF}$, P1 R-NSCs, FACS purified Forse1$^-$ P1 R-NSCs, or P2 R-NSC-derived midbrain dopamine neuron cultures]Perrier et al. 2004]) and into the ventral spinal cord (P2 R-NSCs derived motoneuron cultures [Lee et al. 2007]) as described previously. For neural plate dissection, E8.25 embryos were isolated from Swiss Webster mice. Neural plates were mechanically dispersed into small colonies, plated on Po/Lam/fibronectin-coated dishes, and maintained in N2 medium supplemented with Shh/Dll4/Jag.

Derivation of neural rosettes from mouse ESCs

Mouse ESCs (CJ7, R1) were neurally induced using a modified SFEB protocol (Watanabe et al. 2005). Cells were plated on ultralow adherence dishes (Costar) in KSR/N2 medium (1:1) for 5 d. At day 5, SFEBs were dissociated following 1 h of incubation in Ca^2/Mg^2-free HBSS, replated at 400×10^3 cells per square centimeter on Po/Lam/fibronectin-coated dishes, and maintained in N2 medium with factors as described in the text. After an additional 6 d, cultures were fixed and analyzed by immunocytochemistry for ZO-1$^+$ lumens and rosette markers. Mouse ESCs (CJ7, R1) were neurally induced using a modified SFEB protocol (Watanabe et al. 2005).

Acknowledgments

We are grateful to R. Lovell-Badge, F. Vaccarino, T. Jessell, and C. Henderson for Sox1, Otx2, and HoxA5 antibodies, and other reagents. We also thank M. Tomishima, S. Desbordes, and H. Lee for critical review of the manuscript; J. Hendrikx for cell sorting; and N. Deane, H. Kim, D. Placantonakis, N. Salib, and Y. Ganat for technical assistance. This work was supported by the Kinetics Foundation and the Starr Foundation.

References

Alvarez Buylla, A., Garcia-Verdugo, J.M., and Tramontin, A.D. 2001. A unified hypothesis on the lineage of neural stem cells. *Nat. Rev. Neurosci.* **2:** 287–293.

Androutsellis-Theotokis, A., Leker, R.R., Soldner, F., Hoeppner, D.J., Ravin, R., Poser, S.W., Rueger, M.A., Bae, S.K., Kittappa, R., and McKay, R.D. 2006. Notch signalling regulates stem cell numbers in vitro and in vivo. *Nature* **442:** 823–826.

Artavanis-Tsakonas, S., Rand, M.D., and Lake, R.J. 1999. Notch signaling: Cell fate control and signal integration in development. *Science* **284:** 770–776.

Barberi, T., Klivenyi, P., Calingasan, N.Y., Lee, H., Kawamata, H., Loonam, K., Perrier, A.L., Bruses, J., Rubio, M.E., Topf, N., et al. 2003. Neural subtype specification of fertilization and nuclear transfer embryonic stem cells and application in Parkinsonian mice. *Nat. Biotechnol.* **21:** 1200–1207.

Barberi, T., Bradbury, M., Dincer, Z., Panagiotakos, G., Socci, N.D., and Studer, L. 2007. Derivation of engraftable skeletal myoblasts from human embryonic stem cells. *Nat. Med.* **13:** 642–648.

Bibel, M., Richter, J., Schrenk, K., Tucker, K.L., Staiger, V., Korte, M., Goetz, M., and Barde, Y.A. 2004. Differentiation of mouse embryonic stem cells into a defined neuronal lineage. *Nat. Neurosci.* **7:** 1003–1009.

Bixby, S., Kruger, G.M., Mosher, J.T., Joseph, N.M., and Morrison, S.J. 2002. Cell-intrinsic differences between stem cells from different regions of the peripheral nervous system regulate the generation of neural diversity. *Neuron* **35:** 643–656.

Buaas, F.W., Kirsh, A.L., Sharma, M., Mclean, D.J., Morris, J.L., Griswold, M.D., de Rooij, D.G., and Braun, R.E. 2004. Plzf is required in adult male germ cells for stem cell self-renewal. *Nat. Genet.* **36:** 647–652.

Caldwell, M.A., He, X.L., Wilkie, N., Pollack, S., Marshall, G., Wafford, K.A., and Svendsen, C.N. 2001. Growth factors regulate the survival and fate of cells derived from human neurospheres. *Nat. Biotechnol.* **19:** 475–479.

Conti, L., Pollard, S.M., Gorba, T., Reitano, E., Toselli, M., Biella, G., Sun, Y.R., Sanzone, S., Ying, Q.L., Cattaneo, E., et al. 2005. Niche-independent symmetrical self-renewal of a mammalian tissue stem cell. *PLoS Biol.* **3:** 1594–1606. doi: 10.1371/journal.bio.0030283.

Cook, M., Gould, A., Brand, N., Davies, J., Strutt, P., Shaknovich, R., Licht, J., Waxman, S., Chen, Z., and Gluecksohn-Waelsch, S. 1995. Expression of the zinc-finger gene PLZF at rhombomere boundaries in the vertebrate hindbrain. *Proc.*

Natl. Acad. Sci. **92:** 2249–2253.
Costoya, J.A., Hobbs, R.M., Barna, M., Cattoretti, G., Manova, K., Sukhwani, M., Orwig, K.E., Wolgemuth, D.J., and Pandolfi, P.P. 2004. Essential role of Plzf in maintenance of spermatogonial stem cells. *Nat. Genet.* **36:** 653–659.
Ferrari, D., Sanchez-Pernaute, R., Lee, H., Studer, L., and Isacson, O. 2006. Transplanted dopamine neurons derived from primate ES cells preferentially innervate DARPP-32 striatal progenitors within the graft. *Eur. J. Neurosci.* **24:** 1885–1896.
Gage, F.H. 2000. Mammalian neural stem cells. *Science* **287:** 1433–1438.
Gaiano, N., Nye, J.S., and Fishell, G. 2000. Radial glial identity is promoted by Notch1 signaling in the murine forebrain. *Neuron* **26:** 395–404.
Geny, C., Naimi-Sadaoui, S., Jeny, R., Belkadi, A.M., Juliano, S.L., and Peschanski, M. 1994. Long-term delayed vascularization of human neural transplants to the rat brain. *J. Neurosci.* **14:** 7553–7562.
Goodrich, L.V., Milenkovic, L., Higgins, K.M., and Scott, M.P. 1997. Altered neural cell fates and medulloblastoma in mouse patched mutants. *Science* **277:** 1109–1113.
Gotz, M. and Barde, Y.A. 2005. Radial glial cells: Defined and major intermediates between embryonic stem cells and CNS neurons. *Neuron* **46:** 369–372.
Grignani, F., De Matteis, S., Nervi, C., Tomassoni, L., Gelmetti, V., Cioce, M., Fanelli, M., Ruthardt, M., Ferrara, F.F., Zamir, I., et al. 1998. Fusion proteins of the retinoic acid receptor-α recruit histone deacetylase in promyelocytic leukaemia. *Nature* **391:** 815–818.
Ishibashi, M. and McMahon, A.P. 2002. A sonic hedgehog-dependent signaling relay regulates growth of diencephalic and mesencephalic primordia in the early mouse embryo. *Development* **129:** 4807–4819.
Itoh, M., Nagafuchi, A., Yonemura, S., Kitani-Yasuda, T., Tsukita, S., and Tsukita, S. 1993. The 220-kD protein colocalizing with cadherins in non-epithelial cells is identical to ZO-1, a tight junction-associated protein in epithelial cells: cDNA cloning and immunoelectron microscopy. *J. Cell Biol.* **121:** 491–502.
Jain, M., Armstrong, R.J., Tyers, P., Barker, R.A., and Rosser, A.E. 2003. GABAergic immunoreactivity is predominant in neurons derived from expanded human neural precursor cells in vitro. *Exp. Neurol.* **182:** 113–123.
James, D., Noggle, S.A., Swigut, T., and Brivanlou, A.H. 2006. Contribution of human embryonic stem cells to mouse blastocysts. *Dev. Biol.* **295:** 90–102.
Jessell, T.M. 2000. Neuronal specification in the spinal cord: Inductive signals and transcriptional codes. *Nat. Rev. Genet.* **1:** 20–29.
Johe, K.K., Hazel, T.G., Müller, T., Dugich-Djordjevic, M.M., and McKay, R.D.G. 1996. Single factors direct the differentiation of stem cells from the fetal and adult central nervous system. *Genes & Dev.* **10:** 3129–3140.
Klezovitch, O., Fernandez, T.E., Tapscott, S.J., and Vasioukhin, V. 2004. Loss of cell polarity causes severe brain dysplasia in Lgl1 knockout mice. *Genes & Dev.* **18:** 559–571.
Kruger, G.M., Mosher, J.T., Bixby, S., Joseph, N., Iwashita, T., and Morrison, S.J. 2002. Neural crest stem cells persist in the adult gut but undergo changes in self-renewal, neuronal subtype potential, and factor responsiveness. *Neuron* **35:** 657–669.
Kurokawa, M., Mitani, K., Irie, K., Matsuyama, T., Takahashi, T., Chiba, S., Yazaki, Y., Matsumoto, K., and Hirai, H. 1998. The oncoprotein Evi-1 represses TGF-β signalling by inhibiting Smad3. *Nature* **394:** 92–96.
LaBonne, C. and Bronner-Fraser, M. 1999. Molecular mechanisms of neural crest formation. *Annu. Rev. Cell Dev. Biol.* **15:** 81–112.
Lee, H.J., AlShamy, G., Elkabetz, Y., Schoefield, C., Harrison, N.L., Panagiotakos, G., Tabar, V., and Studer, L. 2007. Directed differentiation and transplantation of human embryonic stem cell derived motoneurons. *Stem Cells* **25:** 1931–1939.
Li, X.J., Du, Z.W., Zarnowska, E.D., Pankratz, M., Hansen, L.O., Pearce, R.A., and Zhang, S.C. 2005. Specification of motoneurons from human embryonic stem cells. *Nat. Biotechnol.* **23:** 215–221.
Machold, R., Hayashi, S., Rutlin, M., Muzumdar, M.D., Nery, S., Corbin, J.G., Gritli-Linde, A., Dellovade, T., Porter, J.A., Rubin, L.L., et al. 2003. Sonic hedgehog is required for progenitor cell maintenance in telencephalic stem cell niches. *Neuron* **39:** 937–950.
Morishita, K., Parganas, E., William, C.L., Whittaker, M.H., Drabkin, H., Oval, J., Taetle, R., Valentine, M.B., and Ihle, J.N. 1992. Activation of EVI1 gene expression in human acute myelogenous leukemias by translocations spanning 300–400 kilobases on chromosome band 3q26. *Proc. Natl. Acad. Sci.* **89:** 3937–3941.
Nagai, T., Aruga, J., Takada, S., Gunther, T., Sporle, R., Schughart, K., and Mikoshiba, K. 1997. The expression of the mouse Zic1, Zic2, and Zic3 gene suggests an essential role for Zic genes in body pattern formation. *Dev. Biol.* **182:** 299–313.
Pankratz, M.T., Li, X.J., Lavaute, T.M., Lyons, E.A., Chen, X., and Zhang, S.C. 2007. Directed neural differentiation of human embryonic stem cells via an obligated primitive anterior stage. *Stem Cells* **25:** 1511–1520.
Perrier, A.L., Tabar, V., Barberi, T., Rubio, M.E., Bruses, J., Topf, N., Harrison, N.L., and Studer, L. 2004. Derivation of midbrain dopamine neurons from human embryonic stem cells. *Proc. Natl. Acad. Sci.* **101:** 12543–12548.
Pittenger, M.F., Mackay, A.M., Beck, S.C., Jaiswal, R.K., Douglas, R., Mosca, J.D., Moorman, M.A., Simonetti, D.W., Craig, S., and Marshak, D.R. 1999. Multilineage potential of adult human mesenchymal stem cells. *Science* **284:** 143–147.
Prada, F.A., Dorado, M.E., Quesada, A., Prada, C., Schwarz, U., and de la Rosa, E.J. 1995. Early expression of a novel radial glia antigen in the chick embryo. *Glia* **15:** 389–400.
Pruszak, J., Sonntag, K.C., Aung, M.H., Sanchez-Pernaute, R., and Isacson, O. 2007. Markers and methods for cell sorting of human embryonic stem cell-derived neural cell populations. *Stem Cells* **25:** 2257–2268.
Reid, A., Gould, A., Brand, N., Cook, M., Strutt, P., Li, J., Licht, J., Waxman, S., Krumlauf, R., and Zelent, A. 1995. Leukemia translocation gene, PLZF, is expressed with a speckled nuclear pattern in early hematopoietic progenitors. *Blood* **86:** 4544–4552.
Roelink, H., Porter, J.A., Chiang, C., Tanabe, Y., Chang, D.T., Beachy, P.A., and Jessell, T.M. 1995. Floor plate and motor neuron induction by different concentrations of the amino-terminal cleavage product of sonic hedgehog autoproteolysis. *Cell* **81:** 445–455.
Roy, N.S., Cleren, C., Singh, S.K., Yang, L., Beal, M.F., and Goldman, S.A. 2006. Functional engraftment of human ES cell-derived dopaminergic neurons enriched by coculture with telomerase-immortalized midbrain astrocytes. *Nat. Med.* **12:** 1259–1268.
Sasai, Y. and De Robertis, E.M. 1997. Ectodermal patterning in vertebrate embryos. *Dev. Biol.* **182:** 5–20.
Shen, Q., Goderie, S.K., Jin, L., Karanth, N., Sun, Y., Abramova, N., Vincent, P., Pumiglia, K., and Temple, S. 2004. Endothelial cells stimulate self-renewal and expand neurogenesis of

neural stem cells. *Science* **304:** 1338–1340.
Shin, S., Mitalipova, M., Noggle, S., Tibbitts, D., Venable, A., Rao, R., and Stice, S.L. 2006. Long-term proliferation of human embryonic stem cell-derived neuroepithelial cells using defined adherent culture conditions. *Stem Cells* **24:** 125–138.
Solecki, D.J., Liu, X.L., Tomoda, T., Fang, Y., and Hatten, M.E. 2001. Activated Notch2 signaling inhibits differentiation of cerebellar granule neuron precursors by maintaining proliferation. *Neuron* **31:** 557–568.
Tabar, V., Panagiotakos, G., Greenberg, E.D., Chan, B.K., Sadelain, M., Gutin, P.H., and Studer, L. 2005. Migration and differentiation of neural precursors derived from human embryonic stem cells in the rat brain. *Nat. Biotechnol.* **23:** 601–606.
Tao, W. and Lai, E. 1992. Telencephalon-restricted expression of BF-1, a new member of the HNF-3/fork head gene family, in the developing rat brain. *Neuron* **8:** 957–966.
Tole, S., Kaprielian, Z., Ou, S.K., and Patterson, P.H. 1995. FORSE-1: A positionally regulated epitope in the developing rat central nervous system. *J. Neurosci.* **15:** 957–969.
Tropepe, V., Hitoshi, S., Sirard, C., Mak, T.W., Rossant, J., and van der Kooy, D. 2001. Direct neural fate specification from embryonic stem cells: A primitive mammalian neural stem cell stage acquired through a default mechanism. *Neuron* **30:** 65–78.
Watanabe, K., Kamiya, D., Nishiyama, A., Katayama, T., Nozaki, S., Kawasaki, H., Watanabe, Y., Mizuseki, K., and Sasai, Y. 2005. Directed differentiation of telencephalic precursors from embryonic stem cells. *Nat. Neurosci.* **8:** 288–296.
Wechsler-Reya, R.J. and Scott, M.P. 1999. Control of neuronal precursor proliferation in the cerebellum by sonic hedgehog. *Neuron* **22:** 103–114.
Wichterle, H., Lieberam, I., Porter, J.A., and Jessell, T.M. 2002. Directed differentiation of embryonic stem cells into motor neurons. *Cell* **110:** 385–397.
Wu, K., Yang, Y., Wang, C., Davoli, M.A., D'Amico, M., Li, A., Cveklova, K., Kozmik, Z., Lisanti, M.P., Russell, R.G., et al. 2003. DACH1 inhibits transforming growth factor-β signaling through binding Smad4. *J. Biol. Chem.* **278:** 51673–51684.
Yamada, T., Pfaff, S.L., Edlund, T., and Jessell, T.M. 1993. Control of cell pattern in the neural tube: Motor neuron induction by diffusible factors from notochord and floor plate. *Cell* **73:** 673–686.
Ye, W.L., Shimamura, K., Rubenstein, J.R., Hynes, M.A., and Rosenthal, A. 1998. FGF and Shh signals control dopaminergic and serotonergic cell fate in the anterior neural plate. *Cell* **93:** 755–766.
Zhang, S.C., Wernig, M., Duncan, I.D., Brustle, O., and Thomson, J.A. 2001. In vitro differentiation of transplantable neural precursors from human embryonic stem cells. *Nat. Biotechnol.* **19:** 1129–1133.

Erratum

Genes & Development 22: 152–165 (2008)

Human ES cell-derived neural rosettes reveal a functionally distinct early neural stem cell stage
Yechiel Elkabetz, Georgia Panagiotakos, George Al Shamy, Nicholas D. Socci, Viviane Tabar, and Lorenz Studer

In the above-mentioned paper, the authors missed a reference (Lazzari et al. 2006) relevant to the current manuscript. On page 161, in the left column, the second paragraph should read as follows:

The prospective isolation of Forse1$^+$/N-cad$^+$ R-NSCs enabled us to demonstrate respecification of anterior BF1$^+$ neuroectodermal cells toward caudal fates including spinal motoneurons and midbrain dopamine neurons. Forse1 could become a powerful tool to isolate NSC populations with anterior CNS bias at various stages of development to probe developmental competency. Default acquisition of anterior neural fate observed in R-NSCs is reminiscent of the anterior neural default model postulated in classical studies of *Xenopus* CNS development. These studies showed that anterior CNS fates are established first and are followed by caudal transformation in response to secreted signals (for review, see Sasai and De Robertis 1997). Forse1$^-$/N-cad$^+$ R-NSCs correspond to posterior regions of the neuroepithelium with the capacity to generate neural crest lineages. Neural crest differentiation potential reflects the early developmental stage and broad differentiation potential of R-NSCs, as neural crest specification in vivo occurs at the neural plate stage (Yamada et al. 1993; LaBonne and Bronner-Fraser 1999). Interestingly, differentiation toward putative neural crest derivatives has been reported previously in a culture system where neural rosettes are derived directly from cloned bovine blastocysts (Lazzari et al. 2006). The isolation of Forse1$^-$ R-NSCs provides a novel strategy for studying early human neural crest development in vitro. Neural crest potential of R-NSCs also points to the importance of monitoring neural crest fates in studies aimed at the generation of defined CNS derivatives. Forse1$^+$ cells lack neural crest markers but retain the plasticity toward neural crest fates upon exposure to caudalizing cues that suppress anterior CNS identity.

In addition, the following reference should have been added to the Reference section:

Lazzari, G., Colleoni, S., Giannelli, S.G., Brunetti, D., Colombo, E., Lagutina, I., Galli, C., and Broccoli, V. 2006. Direct derivation of neural rosettes from cloned bovine blastocysts: A model of early neurulation events and neural crest specification in vitro. *Stem Cells* **24:** 2514–2521.

The authors regret this omission.

Human ES cell-derived neural rosettes reveal a functionally distinct early neural stem cell stage

Yechiel Elkabetz, Georgia Panagiotakos, George Al Shamy, et al.

Genes Dev. 2008, **22:**
Access the most recent version at doi:10.1101/gad.1616208